

PKS 1004+13: A HIGH INCLINATION, HIGHLY ABSORBED RADIO-LOUD QSO – THE FIRST RADIO-LOUD BAL QSO AT LOW REDSHIFT?¹

BEVERLEY J. WILLS², W. N. BRANDT³ & A. LAOR⁴

Draft version October 11, 2018

ABSTRACT

The existence of BAL outflows in only radio-quiet QSOs was thought to be an important clue to mass ejection and the radio-loud – radio-quiet dichotomy. Recently a few radio-loud BAL QSOs have been discovered at high redshift. We present evidence that PKS 1004+13 is a radio-loud BAL QSO. It would be the first known at low-redshift ($z_{\text{em}} = 0.24$), and one of the most radio luminous. For PKS 1004+13, there appear to be broad absorption troughs of O VI, NV, Si IV, and C IV, indicating high-ionization outflows up to $\sim 10\,000$ km s⁻¹. There are also two strong, broad (~ 550 km s⁻¹), high ionization, associated absorption systems that show partial covering of the continuum source. The strong UV absorption we have detected suggests that the extreme soft-X-ray weakness of PKS 1004+13 is primarily the result of absorption. The large radio-lobe dominance indicates BAL and associated gas at high inclinations to the central engine axis, perhaps in a line-of-sight that passes through an accretion disk wind.

Subject headings: quasars: absorption lines — quasars: emission lines — quasars: individual (PKS 1004+13) — UV: galaxies — X-rays: galaxies

1. INTRODUCTION

About 11% of radio-quiet QSOs show strong broad absorption troughs (BALs) displaced to the blue of the corresponding broad emission lines of O VI $\lambda 1034$, Ly α , NV $\lambda 1240$, Si IV $\lambda 1400$, and C IV $\lambda 1549$, indicating high-ionization outflows up to 0.1c – 0.2c. Except for the absorption, the ultraviolet spectra of BAL QSOs are very similar to non-BAL QSOs. This, together with limits on resonance photons scattered into the absorption troughs, and partial covering deduced from spectropolarimetry and absorption-line ratios, suggests that BAL outflows are common to all (radio-quiet) QSOs, but are recognized only when BAL material intercepts our line-of-sight. BALs appeared to be a unique property of radio-quiet QSOs. Seemingly this was an important clue to central engine physics: QSOs appear to produce either a highly collimated, powerful, relativistic jet, or a sub-relativistic uncollimated wind that accelerates BAL clouds, but not both (Stoche et al. 1992, Weymann 1997). Recently, with the advent of systematic identification of faint (mJy) radio sources at 1.4GHz, several radio-loud BAL QSOs have been discovered, so the incidence of BALs no longer changes at the conventional limit separating radio-quiet and radio-loud QSOs (Brotherton et al. 1998a; Becker et al. 1999). Nevertheless, BAL properties probably still provide important clues to the production of powerful radio jets (Weymann 1997), and the axis defined by powerful radio jets may be used to relate the geometry of BAL regions to the symmetry axis of the central engine.

Another clue to the physics of mass ejection in BAL

QSOs, and therefore perhaps in all QSOs, is the extreme weakness of their soft X-ray fluxes (0.2keV–2keV; Green et al. 1995; Green & Mathur 1996); even their more penetrating harder X-rays are extremely weak (2keV–10keV, Gallagher et al. 1999). In order to understand the nature of soft X-ray weak (SXW) QSOs, that is, those having $\alpha_{\text{ox}} > 2$ (3000Å to 2keV), we have investigated the UV spectra of all PG QSOs with archival IUE and HST ultraviolet spectra (Brandt et al. 1999). PKS 1004+13 is a member of that sample, and is also the only radio-loud, X-ray-weak member.

PKS 1004+13 (4C 13.41, PG 1004+130) is a $V=15.2^m$, QSO of low redshift, $z = 0.240$, thus $M_B = -25.6^5$. It is a classic powerful lobe-dominant radio source – 1.2 Jy at 1.4GHz, or $\log L_{1.4\text{GHz}} \sim 33.6$ erg s⁻¹ Hz⁻¹, with radio-loudness, $\log R^* = 2.32$ (as defined by Sramek & Weedman 1980). Elvis & Fabbiano (1984) noted its exceptionally weak X-ray emission, deriving a spectral index > 2.01 between 2500Å and 2keV. They favored an explanation in terms of an exceptionally strong optical-ultraviolet Big Blue Bump, rather than absorption of the X-rays. They also suggested that a relatively weak EUV ionizing continuum could result in weak BLR emission. Here we present and discuss evidence that PKS 1004+130 is not only a powerful radio source, but also a BAL QSO.

2. OBSERVATIONS & MEASUREMENTS

We have retrieved and combined the NEWSIPS-calibrated IUE data from the short-wavelength camera, including our own IUE observation (SWP04942, SWP10850,

¹Based partly on observations by the International Ultraviolet Explorer satellite, collected at the Villafranca Satellite Tracking Station of the European Space Agency.

²McDonald Observatory & Astronomy Department, University of Texas at Austin, TX 78712, USA; bev@astro.as.utexas.edu

³Department of Astronomy & Astrophysics, 525 Davey Laboratory, Pennsylvania State University, University Park, PA 16802; niel@astro.psu.edu

⁴Department of Physics, Technion, Israel Institute of Technology, Haifa 32000, Israel; laor@physics.technion.ac.il

⁵ $H_0 = 50$ km s⁻¹ Mpc⁻¹, and $q_0 = 0$.

SWP16824, SWP27517 with observation dates UT 1979 April 15, 1980 Dec. 1, 1982 April 24, 1986 Jan. 12 respectively), weighting these according to the square of the signal-to-noise ratio. All observations were at low dispersion in the large aperture, giving a resolution of $\sim 1100 \text{ km s}^{-1}$ from 1170\AA to 1980\AA . Wavelength scales were checked using the geocoronal $\text{Ly}\alpha$ line. We have applied an approximate correction for IUE artifacts and the wings of the geocoronal $\text{Ly}\alpha$ line, by subtracting the SWP artifact spectrum appropriate to point source spectral extraction, as presented by Crenshaw, Bruegman, & Norman (1990).

By good fortune, the line-of-sight to PKS 1004+13 happens to pass only $34'$ from the center of the Leo I dwarf spheroidal galaxy, so Bowen et al. (1997) used this QSO as a background probe of Leo I's halo. They obtained high-resolution ($0.14\text{\AA pixel}^{-1}$) HST GHRS spectra of PKS 1004+13 from 1276\AA to 1562\AA . We have retrieved the HST archival spectra, applying the same wavelength shift as Bowen et al. to convert to a heliocentric velocity scale.

Both the shape and flux density level of the GHRS spectrum agree well with the IUE spectrum, suggesting the correctness of the flux-density calibration, despite the possibility of a 1500\AA (observed wavelength) bump artifact in the IUE SWP data (Kinney et al. 1991).

3. RESULTS

The HST and coadded IUE spectrum for PKS 1004+13 is shown as the lower spectrum in Figure 1. Beneath is a standard deviation spectrum derived from the scatter among the individual IUE spectra. The systemic redshift $z_{\text{em}} = 0.2401$ is derived from our and Stockton & MacKenty's (1987) measured wavelength of the narrow [O III] $\lambda 5007$ emission line. Based on this, above the spectrum are shown the expected wavelengths of redshifted broad emission lines. As noted by Kinney et al. (1991): "Based on this spectrum alone, 1004+130 would not be classified as a QSO because of the very weak $\text{Ly}\alpha$ emission line." Even the expected strong CIV $\lambda 1549$ emission is not clearly present. To demonstrate the unusual weakness of the broad $\text{Ly}\alpha$ emission, we note that its rest equivalent width $\text{EW} = 17\text{\AA}$ is the smallest of 19 low-redshift, radio-loud, lobe-dominant QSOs from the HST archives. The mean for this sample is 140\AA . The next smallest $\text{EW}(\text{Ly}\alpha)$ is 56\AA for 3C 288.1, for which strong associated absorption is clearly present (Wills et al. 1995). Below, we compare the UV spectrum of PKS 1004+13 with that of a typical QSO.

Kinney et al. (1991) noted unresolved absorption features at 1534\AA and 1919\AA that they attributed to NV and CIV doublets at a redshift of 0.24. The high-resolution, high signal-to-noise-ratio GHRS spectrum shows that the components of the NV $\lambda\lambda 1238, 1242$ doublet are further split and that there is corresponding strong absorption in O VI $\lambda\lambda 1032, 1038$ (Fig. 2a, b). These two absorption systems are also seen, but less clearly, in $\text{Ly}\alpha$ (Fig. 2c). All these features are also marked beneath the spectrum of Fig. 1. These systems have heliocentric absorption redshifts of $z_a = 0.2364$ and 0.2387 , and are intrinsically broad – respectively $\sim 600 \text{ km s}^{-1}$ and 500 km s^{-1} total

width, representing outflows of $50 \pm 50 \text{ km s}^{-1}$ (no outflow) to 1200 km s^{-1} . It is therefore not surprising that the corresponding high-ionization emission lines should be suppressed over this velocity range. There is no sign of low-ionization absorption at these redshifts in the broad Mg II $\lambda 2798$ emission line (Antonucci, Wills, unpublished). Both O VI doublets appear optically thick ($\tau_{1034\text{\AA}} \sim 6$), with absorbing gas covering only 70% to 80% of the continuum source (using the method of Arav et al. 1999). Thus the absorption is intrinsic to the QSO. The result for the NV doublets are consistent, but with larger uncertainties.

We also note the probable existence of broad absorption troughs at even greater outflow velocities – up to $\sim 10000 \text{ km s}^{-1}$. The wavelength range corresponding to 0 to -10000 km s^{-1} is indicated by shading in Figure 1, for O VI $\lambda 1034$, $\text{Ly}\alpha$, NV $\lambda 1240$, Si IV $\lambda 1397$, and CIV $\lambda 1549$. The CIV associated and broader absorption are visible on the IUE two-dimensional images for the 3 long-exposure spectra. These BAL-like troughs suggest a reason why the $\text{Ly}\alpha$ -NV $\lambda 1240$ broad emission is so weak: it has been suppressed largely by NV absorption. The $\text{Ly}\alpha$ BAL would appear to be much weaker than for the higher ionization species. Above the PKS 1004+13 spectrum, we show for comparison a spectrum of the well-known BAL QSO, PG 0946+301 (Korista & Arav 1997), redshifted to align the broad absorption features as indicated by the shaded strips. Note the suppression of broad $\text{Ly}\alpha$ emission by the NV BAL for PG 0946+301. Higher quality UV spectroscopy would confirm the reality of BALs in PKS 1004+13.

One way in principle to distinguish absorption from emission, and isolate the absorption spectrum of PKS 1004+13, is to divide by a 'normal' QSO spectrum. We and others (e.g., Wills et al. 1999) have shown that the greatest spectrum-to-spectrum differences can be described by luminosity relationships (the Baldwin effect), dependence on Boroson and Green's (1992) optical Principal Component 1 (PC1), and radio core-dominance (Baker & Hunstead 1995, Vestergaard 1998). Therefore we choose to divide by a QSO spectrum that is quite similar in luminosity, radio core-dominance, and in optical PC1 properties. We chose 3C 263⁶, with $\text{EW}(\text{Ly}\alpha) = 114\text{\AA}$, and $\text{EW}(\text{CIV}) = 86\text{\AA}$, from a sample of radio-loud QSOs (Wills et al. 1995). Figure 3 shows the result, and serves to illustrate the approximate strength of the NV absorption. This technique would give an accurate absorption profile only if the template spectrum were an accurate match to the emission line spectrum of PKS 1004+13, and in the unlikely situation that the absorbing gas covered the continuum and the whole of the emission line region. Note that if the broad absorption in PKS 1004+13 had been further blueshifted, as in many well-known BAL QSOs, it would have been more clearly seen against a well-defined continuum.

4. DISCUSSION

PKS 1004+13 shows the following characteristics typical of QSOs with high-ionization BALs: (i) absorption to

⁶For PKS 1004+13, $M_B = -25.6$, and core-dominance = -1.7 (§4). Optical PC1 properties are: $\text{FWHM}(\text{H}\beta)$, 6300 km s^{-1} ; $\text{EW}([\text{O III}])$, 6\AA ; $[\text{O III}]/\text{H}\beta$ intensity ratio, 0.15; and $\text{H}\beta$ asymmetry, 0.06 (Boroson & Green 1992). For 3C 263, $M_B = -27.0$; radio core-dominance, -1.1 ; $\text{FWHM}(\text{H}\beta)$, 6100 km s^{-1} ; $\text{EW}([\text{O III}])$, 17\AA ; $[\text{O III}]/\text{H}\beta$ intensity ratio, 0.24; $\text{H}\beta$ asymmetry -0.1 .

high outflow velocities ($\sim 10\,000\text{ km s}^{-1}$) in high-ionization lines of O VI, NV, CIV, and possibly Si IV, with a weak Ly α broad absorption, and suppression of the broad Ly α emission line, (ii) judging by the region of the NV ‘trough’ in the high-resolution GHRS spectrum, the troughs are smooth; probably the CIV seen only in low-resolution IUE spectra will not resolve out in higher resolution observations, (iii) we measure a non-zero balnicity index, 850 km s^{-1} (cf. Weymann et al. 1991), (iv) there are multiple (2), high-ionization associated absorption systems, as commonly go along with BAL absorption (e.g., Ogle et al. 1999), (v) it is extremely weak in soft X-rays, as in other BAL QSOs (Green et al. 1995; Green & Mathur 1996), (vi) there is scattered-light polarization (see below), and (vii) there is no sign of continuum reddening (Figure 7 of Elvis & Fabbiano 1984).

Unlike any BAL QSOs reported in the literature⁷, PKS 1004+13 shows classical lobe-dominant radio structure (Kellermann et al. 1994, Miley & Hartsuijker 1978), with core dominance, $\log(\text{core flux/lobe flux}) = -1.74$ (5GHz, rest frame). Thus, for the first time, it may be possible to relate BAL QSO properties to the axis of the central engine. To put the core-dominance in context we note that PKS 1004+13 is also a 4C radio source, selected at a low frequency, 178MHz. We can compare the core-dominance with the distribution for 3CR sources, also selected at 178MHz, as this quantity is distributed similarly for all FR II radio sources in 3CR and 4C (Hoekstra, Barthel, & Hes 1997). Of 28 3CR QSOs with sufficient radio imaging, only two have clearly smaller core-dominance – 3CR 68.1, an extremely reddened and highly scattering-polarized QSO with strong associated absorption (Brotherton et al. 1998b), and 3CR 351 – with strong absorption by ionized gas in the X-rays and strong, high-ionization, associated absorption lines in the UV (Mathur et al. 1994). Of 66 3CR radiogalaxies, half have smaller core-dominance. Thus, in unified schemes for radio sources, this indicates for PKS 1004+13 an inclination angle skimming the dusty torus, $\sim 50^\circ$. Thus, the BAL region in PKS 1004+13 appears to lie at a large angle to the central engine’s axis, and the BALs could arise in an equatorial accretion disk wind. This also ties in with pictures of the polarization scattering geometry in which BAL gas lies at low disk latitudes.

About a third of BAL QSOs show polarization at the $\gtrsim 2\%$ level, but this is rare in UV-selected non-BAL QSOs. Polarization increases towards the blue as expected for scattered light (Schmidt & Hines 1999). PKS 1004+13 shows continuum polarization at the $\sim 2\%$ level, increasing towards the blue (Antonucci et al. 1996; Stockman, Moore, & Angel 1984). The scattered-light geometry suggested by this polarization may be related to the partial covering of the continuum that we deduce for the O VI absorbing region; partial covering has been shown directly by changes in polarization across the absorption troughs of some radio-quiet BAL QSOs (Schmidt & Hines 1999).

PKS 1004+13 could have provided an interesting test of scattering geometry for BAL QSOs, through a comparison of the polarization position angle with the position angle of the radio axis (117°). Unfortunately, the optical position angle is ill-defined at present. Antonucci et al. and Stockman et al. both find different and wavelength-dependent polarization position angles, suggesting variability, and probably more than one polarization mechanism.

Is the discovery of BALs in PKS 1004+13 consistent with the 11% rate of occurrence among radio-quiet QSOs (Weymann 1997) or among radio-loud QSOs discovered in deep radio surveys? We can address this question by noting that Brandt et al. (1999) have searched for associated absorption lines in all available HST and IUE spectra with good signal-to-noise ratio, for all $z < 0.5$ QSOs in the PG optically-selected sample. PKS 1004+130 is the only one of 12 radio-loud QSOs to show probable BALs – consistent with the usual discovery rates. Are BAL properties a function of radio-loudness? If strong absorption near z_{em} is a common characteristic, this may explain why more radio-loud BAL QSOs have not been discovered.

PKS 1004+13 is very bright in radio through UV wavelengths, and it is nearby, enabling more detailed spectroscopic follow-up and imaging at high spatial resolution. The low redshift also means that the broad hydrogen lines and narrow line region (NLR) emission lines are accessible in the optical and near infrared. High-quality UV spectroscopy is needed to establish whether PKS 1004+13 is indeed a BAL QSO, and would, in any case, lead to important clues to physics and covering factor of the absorbing outflows, the BLR, and the continuum that ionizes it. Imaging of the relatively bright radio nucleus, polarized (scattered) light and [O III] emission may lead to further clues to the geometry. PKS 1004+13 may therefore be a key AGN in understanding the relationship between radio-loudness and BALs, and the geometry of BAL QSO outflows.

We thank Michael Brotherton for valuable discussions, and Nahum Arav for supplying the data for PG 0946+301. Thanks to Yoji Kondo and Willem Wamsteker for help in arranging the IUE observations, and C. Imhoff and R. Thompson for patient answering of IUE questions. Some data are from the Multimission Archive at the Space Telescope Science Institute (MAST). STScI is operated by the Association of Universities for Research in Astronomy, Inc., under NASA contract NAS5-26555. MAST for non-HST data is supported by the NASA Office of Space Science via grant NAG5-7584 and others. This research has made use of the NASA/IPAC Extragalactic Database (NED), which is operated by the Jet Propulsion Laboratory, Caltech, under contract with NASA. This research is supported by NASA through LTSA grant numbers NAG5-3431 (B.J.W.) and NAG5-8107 (W.N.B.).

⁷Recently, another FR II BAL QSO has been found in the FIRST survey (Becker, private communication).

REFERENCES

- Antonucci, R. R. J., Geller, R., Goodrich, R. W., & Miller, J. S. 1996, *ApJ*, 472, 502
- Arav, N., Korista, K. T., de Kool, M., Junkkarinen, V. T., & Begelman, M. C. 1999, *ApJ*, in press
- Baker, J. C., & Hunstead, R. W. 1995, *ApJ*, 452, L95
- Becker, R. H., White, R. L., Gregg, M. D., Brotherton, M. S., Laurent-Muehleisen, S., & Arav, N. 1999, in preparation
- Bowen, D. V., Tolstoy, E., Ferrara, A., Blades, J. C., & Brinks, E. 1997, *ApJ*, 478, 530
- Boroson, T. A., & Green, R. F. 1992, *ApJS*, 80, 109
- Brandt, W. N., Laor, A., & Wills, B. J. 1999, *ApJ*, submitted
- Brotherton, M. S., Van Breugel, W., Smith, R. J., Boyle, B. J., Shanks, T., Croom, S. M., Miller, L., & Becker, R. H. 1998a, *ApJ*, 505, 7
- Brotherton, M. S., Wills, B. J., Dey, A., Van Breugel, W., & Antonucci, R. R. J. 1998b, *ApJ*, 501, 110
- Crenshaw, D. M., Bruegman, O. W., & Norman, D. J. 1990, *PASP*, 102, 463
- Elvis, M., & Fabbiano, G. 1984, *ApJ*, 280, 91
- Gallagher, S. C., Brandt, W. N., Sambruna, R. M., Mathur, S., & Yamasaki, N. 1999, *ApJ*, in press (astro-ph/9902045)
- Green, P. J., Schartel, N., Anderson, S. F., Hewett, P. C., Foltz, C. B., Brinkmann, W., Fink, H., Truemper, J., & Margon, B. 1995, *ApJ*, 450, 51
- Green, P. J., & Mathur, S. 1996, *ApJ*, 462, 637
- Hoekstra, H., Barthel, P. D., & Hes, R. 1997, *A&A*, 319, 757
- Kellermann K. I., Sramek, R. A., Schmidt, M., Green, R. F., & Shaffer, D. B. 1994, *AJ*, 108, 1163
- Kinney, A. L., Bohlin, R. C., Blades, J. C., & York, D. G. 1991, *ApJS*, 75, 645
- Korista, K. & Arav, N. 1997, in ASP Conf. Ser. 128, Mass Ejection from Active Galactic Nuclei, ed. R. J. Weymann, N. Arav, & I. Shlosman (San Francisco: ASP), 201
- Mathur, S., Wilkes, B., Elvis, M., & Fiore, F. 1994, *ApJ*, 434, 493
- Miley, G. K., & Hartsuijker, A. P. 1978, *A&AS*, 34, 129
- Ogle, P. M., Miller, J. S., Tran, H., Goodrich, R. W., & Martel, A. R. 1999, *ApJS*, in press
- Schmidt, G. D., & Hines, D. C. 1999, *ApJ*, 512, 125
- Sramek, R. A., & Weedman, D. W. 1980, *ApJ*, 238, 435
- Stoche, J. T., Morris, S. L., Weymann, R. J., & Foltz, C. B. 1992, *ApJ*, 396, 487
- Stockman, H. S., Moore, R. L., & Angel, J. R. P. 1984, *ApJ*, 279, 485
- Stockton, A. & MacKenty, J. W. 1987, *ApJ*, 316, 584
- Vestergaard, M. 1998, Ph.D. dissertation, Niels Bohr Institute for Astronomy, Physics, & Geophysics, Copenhagen University Observatory
- Weymann, R. J. 1997, in ASP Conf. Ser. 128, Mass Ejection from Active Galactic Nuclei, ed. R. J. Weymann, N. Arav, & I. Shlosman (San Francisco: ASP), 3
- Weymann, R. J., Morris, S. L., Foltz, C. B., & Hewett, P. C. 1991, *ApJ*, 373, 23
- Wills, B. J., Thompson, K. L., Han, M., Netzer, H., Wills, D., Baldwin, J. A., Ferland, G. J., Browne, I. W. A., & Brotherton, M. S. 1995, *ApJ*, 447, 139
- Wills, B. J., Laor, A., Brotherton, M. S., Wills, D., Wilkes, B. J., Ferland, G. J., & Shang, Zhaohui 1999, *ApJ*, 515, L53

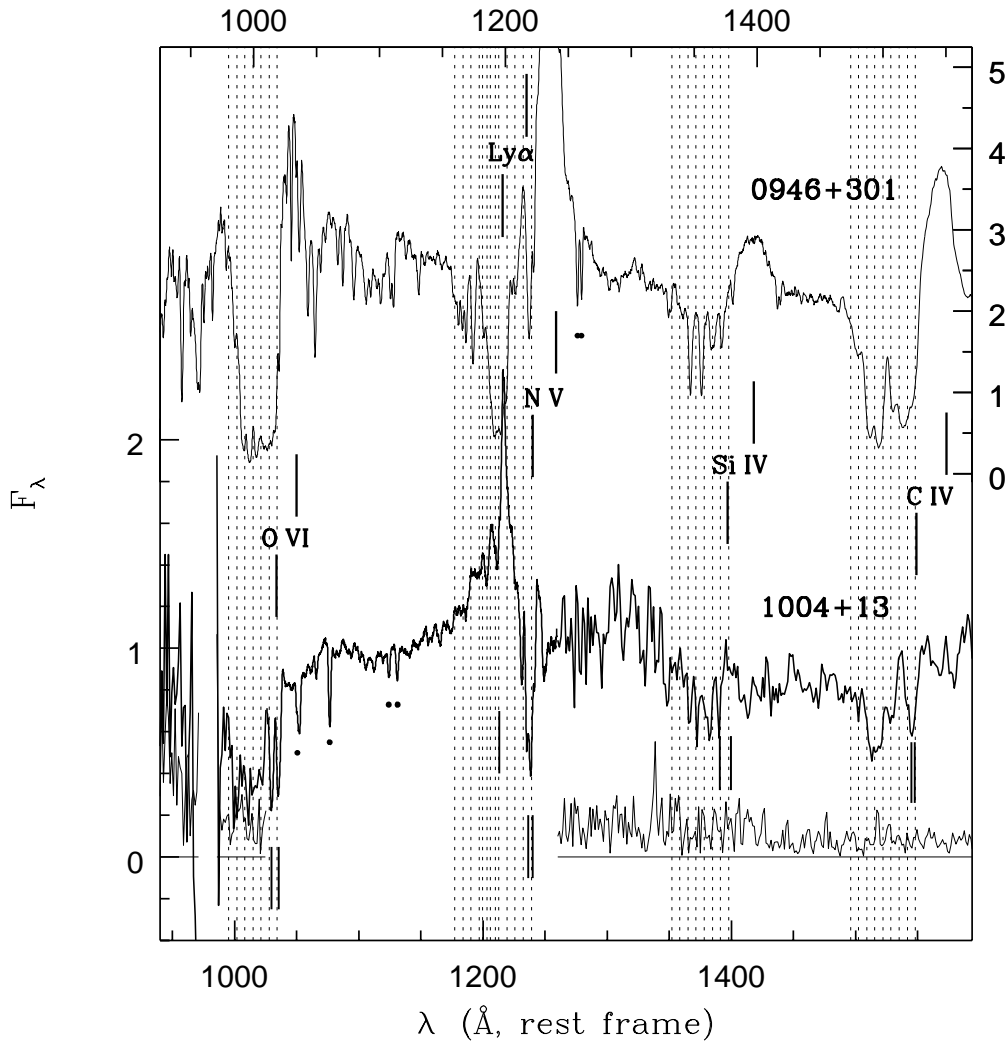


FIG. 1.— Below: The observed ultraviolet spectrum of PKS 1004+13, derived from HST GHRS and IUE SWP data, shown on a rest-wavelength scale. The GHRS data have been smoothed (compare with Fig. 2). The standard deviation spectrum is shown, only for the IUE data. Above: The smoothed HST spectrum of the well-known BAL QSO, PG 0946+301 (Korista & Arav 1997), on a redshifted scale (top) that aligns its BALs with our suggested BALs for PKS 1004+13. The ordinates are in $10^{-14} \text{ erg s}^{-1} \text{ cm}^{-2} \text{ \AA}^{-1}$ and $10^{-15} \text{ erg s}^{-1} \text{ cm}^{-2} \text{ \AA}^{-1}$ for PKS 1004+13 and PG 0946+301, respectively. The BAL velocity range, 0 to $-10,000 \text{ km s}^{-1}$, is indicated by the shading. Note the overlapping troughs of Ly α and NV $\lambda 1240$. The expected wavelengths of emission-line peaks are indicated next to the labels (for PKS 1004+13, $z_{\text{em}} = 0.2401$; for PG 0946+301, $z_{\text{em}} = 1.222$). The expected positions of narrower absorption doublets are shown below the PKS 1004+13 data. Dots show the positions of Milky Way interstellar absorptions. The gap near 980 \AA corresponds to geocoronal Ly α .

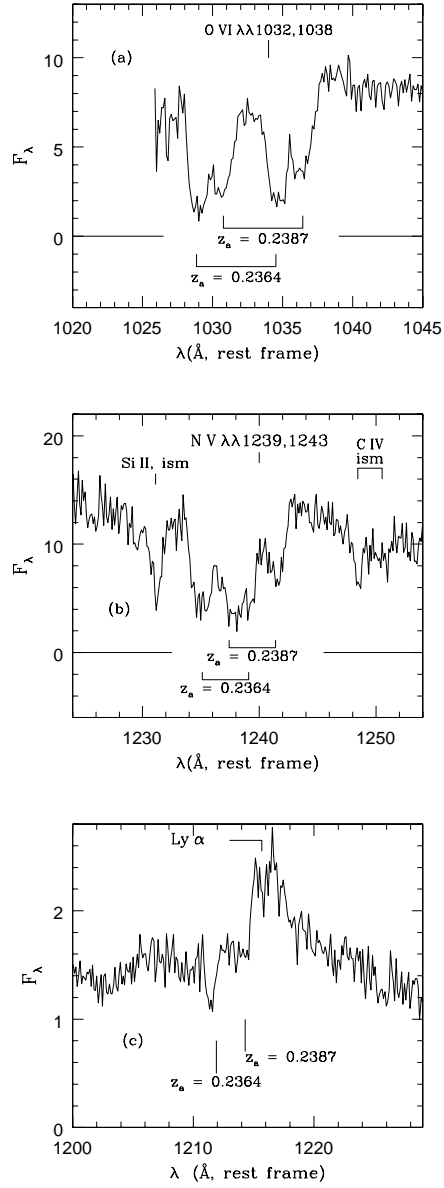


FIG. 2.— The narrower absorption features in PKS 1004+13, illustrating the two redshift systems, and the widths of the absorption features for the wavelength regions of a) O VI, b) NV, and c) Ly α . The expected wavelength of the emission-line peak is indicated above the spectra. The long-wavelength edge of the absorption corresponds to zero rest-frame velocity for the longest wavelength pair of the doublets. For the ordinate scale, see Fig. 1.

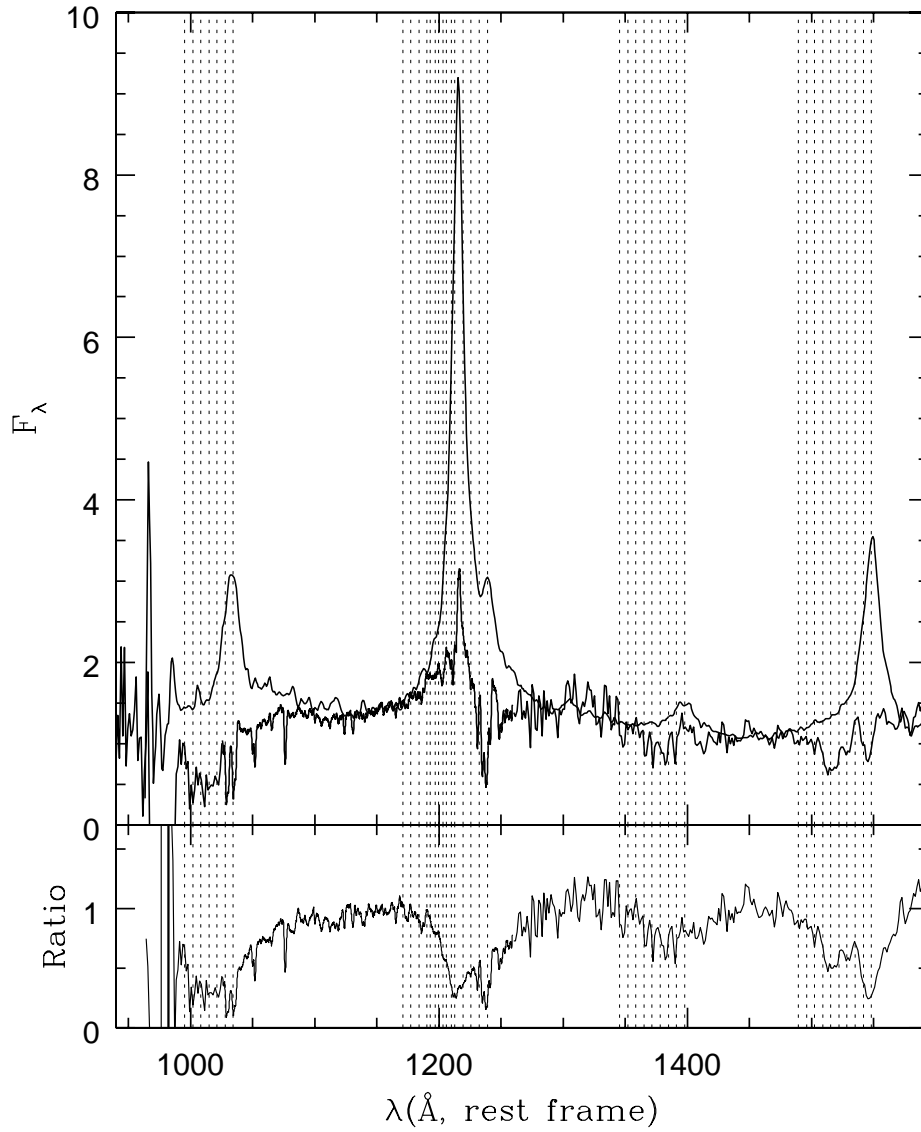


FIG. 3.— Comparison of a smoothed, scaled spectrum of a matched radio-loud QSO 3C 263 (see text) with the ultraviolet spectrum of PKS 1004+13. Both are corrected for Milky Way reddening. In the lower panel we show the division of the spectra, PKS 1004+13 by 3C 263.